Western Region Technical Attachment
No. 06-03
January 31, 2006

Inside Sliders. Part II: Model Forecasts for Inside Sliders and Their Biases

Jim Wallmann
NWSFO Reno, NV

I - Introduction

Inside sliders (Wallmann 2006, hereafter Part I) are mesoscale systems that can produce localized heavy rain and snow along the Sierra Front of Western Nevada. Due to their small scale, numerical models can have difficulty forecasting the systems. This paper will investigate the Global Forecast System (GFS) and North American Mesoscale (NAM, formerly the Eta) model forecasts of inside sliders and typical errors associated with these forecasts. Section II will describe the methodology used in the paper. Section III will look at both GFS and NAM model forecasts for inside sliders while Section IV follows with upstream observational clues that may help forecast an inside slider system. Section V will present a summary and conclusion.

II - Methodology

Five inside slider cases were investigated over the 2004 and 2005 winter seasons, and are listed in Part I. For each of the cases, GFS and NAM forecasts were evaluated based on position and strength of the features described in Part I. In addition, since these systems produce precipitation in most cases, the model QPF fields were compared to observed precipitation, and any systematic signatures in the forecast precipitation fields were noted. Forecasts out to 48 hours were evaluated, but more emphasis was placed on the 12-24 hour forecasts. This was done to better capture model tendencies and biases for inside slider events, since forecasts beyond 24 hours will generally have larger position errors. In addition, mesoscale features that only span a few grid points are lost quickly. Finally, observations from 12-18 hours before the peak of the events were also analyzed which would help make adjustments to, and improve on the model forecasts.

To best illustrate the findings of an average inside slider case, this paper focuses on the forecasts for the January 20, 2004 event. Since the system primarily affected the Sierra Front (Part I) between 08 UTC and 15 UTC, NAM and GFS forecasts from 12 UTC 19 Jan 2004 were used to best illustrate a 24 hour forecast as described above. In the observation section, satellite, radar and surface observations were used up until 00 UTC 20 Jan approximately 12 hours before the event peak. The one exception dealt with upper air observations near Reno, since the 20 Jan 2004 observations were unavailable to due equipment failures. To fill in this gap, the 20 Sep 2004 observations were used, where 20 Sep was a case very similar to 20 Jan, except for the time of year.

III - Model Forecasts

Numerical models can greatly aid the operational forecaster with inside slider events, even when the models do not explicitly forecast the magnitude of an event. The models often handle the synoptic and mesoscale situation well, but sometimes adjustments must be made to mesoscale features not resolved by the models. In such cases, model QPF needs to be adjusted and therefore the sensible weather will be different from the model forecast. This section will look at both the GFS and NAM model forecasts for the inside slider on 20 Jan 2004. The synoptic and mesoscale features described in Part I will be the basis of the analysis and discussion.

a) GFS

Overall, the GFS performed well with the synoptic features of inside sliders. The forecasts of the north-south jet were often well-positioned, and the track of the short wave itself was well handled. However, the short wave itself was occasionally forecast too far east, along with the associated mid-level cold pool (Fig. 1). On 20 January, the position differences compared to upper air observations and the 14 UTC RUC analysis are small but significant. The GFS forecast short wave position, only 100 km or less further east than the actual position, resulted in an increase in 500 mb temperatures of 1-2 C (Fig. 1c and 1d). The result would be that the Sierra Front is forecast to be more stable than what actually occurred. However, even in cases where the GFS handled the features properly that are favorable for precipitation, some adjustments are needed.

For example, with the location of the north-south jet streak into northern California, the Sierra Front would be located in the left exit region of the jet streak, favorable for upward vertical motion. The GFS only shows weak, if any, divergence aloft at the 400 mb and 300 mb layers (Fig. 2) over all of Nevada. While this may be accurate of the synoptic scale which the GFS handles fairly well, precipitation produced by these systems is mesoscale in nature. The GFS resolution of T254 (NOAA-EMC, 2003), analogous to 55 km gridded resolution, is much too broad to accurately represent the strength of the divergence aloft within any convective band that forms. Therefore, if a band is expected to develop, it can be assumed that the divergence aloft will be stronger than depicted by the model in the band itself.

A similar situation arises in dealing with the low-level deformation axis. The GFS resolution is too broad to represent the strength of the convergence within the deformation axis. The GFS often depicts weak convergence in the low levels (Fig. 3 at 700 mb), over a much broader area than is likely occurring. In fact, the GFS shows little if any deformation in the 700 mb wind field at 06 UTC (Fig. 4). This is just the band of precipitation moved over the Sierra Front at 09 UTC and became more widespread. By 12 UTC 20 Jan 2004, only the broad cyclonic flow around the 700 mb low center in southern Nevada can be seen. Another interesting aspect of the wind field however, has to do with the north to northeast 700 mb wind (at 06 UTC and 12 UTC respectively – Fig. 3). As mentioned in Part I, northeast winds create favorable upslope conditions

along the Sierra Front. In addition, Part I also brought up the analogous impacts of a north wind along the Sierra Front as compared to the Wasatch Front (Steenburgh et al. 2003) creating a convergence zone just upstream of the mountains. While the wind field suggests the convergence zone is possible, the GFS still does not show any convergence along the Sierra Front. In fact, the GFS forecasts the greatest convergence near the 700 mb low center at both 06 UTC and 12 UTC. This may be a result of the poor terrain resolution of the GFS, so the synoptic scale convergence near the low center is all that is shown.

The GFS often forecasts the 500 mb cold pool well, which can be see in the Lifted Index (LI – Fig. 5) forecast. However, since the convection tends to be shallow, with cloud tops between 500 and 400 mb, LI values are typically slightly positive, with values less than 4 most conducive to convective snows with inside sliders. The greatest values are to the east of the Sierra Front, which coincides well with the location of the coldest temperatures at 500 mb. Another useful tool described in Part I used to assess the stability of the atmosphere is the High Level Total Totals (HLTT) Index (Milne, 2004). Values greater than 30 C are required for warm season convection, but since the values are skewed higher by colder 500 mb temperatures (Milne 2004), values greater than 32-34 C are needed for cold season convection. While these values are marginal near the Sierra Front with values only 32-34 C (Fig. 5), values greater than 34 C are present within the core of the cold pool over central Nevada. If the HLTT values are adjusted upward by 2-4 C to account for the warm bias in 500 mb temperatures over the Sierra Front, the HLTT values become 36 to 42 C, which are much more conducive to convective precipitation. It is important to note that any index used to assess instability is not complete without an analysis of a current and forecast sounding, which can show shallow layers of instability that are not identified by coarse indices.

Once the aforementioned features are analyzed, a glance at the GFS QPF for each event showed consistent fields that can be adjusted for an inside slider event. The GFS QPF field (Fig. 6) is generally too light and too broad, given the coarse GFS resolution, with QPF of less than a tenth of an inch over much of northwest Nevada. Occasionally, a maximum is shown in the vicinity of Lake Tahoe, which occurred on 20 Jan. In general, the GFS QPF is often only 25-50% of the actual water equivalent measured within the Sierra Front, with the lighter amounts verifying further to the east and west (Table 1 – from Part I. Also see Fig. 11 from Part I.) Therefore, if the forecaster deems the inside slider strong, QPF amounts forecast by the GFS can be safely doubled along the Sierra Front, if not quadrupled when amounts are very light.

b) NAM

The NAM, with its better resolution of 12 km, has the potential to produce a better forecast for mesoscale events such as inside sliders. However, how well it initialized the inside slider short wave has a great impact on its forecasts. (The GFS also has this issue, but with its later start time, the GFS has more observations from the Pacific Ocean which frequently results in a better initialization of the large scale features.) Even with the

better resolution of the NAM, there are some general signatures in the model output that occur often with inside slider systems.

Similar to the GFS, if the NAM initialized well, the individual short wave and the north-south jet streak should be handled well by the NAM in the first 24 to 36 hours. For the 20 Jan case, the NAM position was similar to the GFS, but was weaker with the short wave (Fig. 7). In contrast, the 500 mb temperatures in the mid level cold pool were better

Location	Direction and Distance from the Reno Airport	Precipitation Amount
Reno Airport	0	0.57”
Reno- North Hills	5 mi N	0.24”
Stead, NV	11 mi NW	0.15”
Sparks, NV	4 mi NE	0.34”
SE Sparks, NV	1 mi NE	0.56”
Virginia City, NV	16 mi SE	0.32”
Spanish Springs, NV	9 mi NE	0.38”
Carson City, NV	21 mi S	0.40”
Minden, NV	40 mi S	0.34”
Dagget Pass, NV	39 mi S	0.30”
Glenbrook, NV	30 mi S	0.16”
Fallon NAS, NV	58 mi E	Trace
Gerlach, NV	82 mi N	0.06”
Fernley, NV	31 mi E	0.05”
Markleeville, CA	57 mi S	0.36”
Yerington, NV	49 mi SE	0.04”
Hawthorne, NV	91 mi SE	0.10”
Truckee, CA	22 mi SW	0.20”
Portola, CA	39 mi NW	0.07”
South Lake Tahoe AP, CA	43 mi SSW	0.04”
6 N Smith, NV	47 mi SE	0.66”
Lovelock, NV	77 mi NE	0.03”
4N Topaz Lake, NV	55 mi S	0.15”

Table 1. *Selected locations used in the subjective analysis of Figure 11. Distance from the Reno airport, elevation, and liquid equivalent precipitation amount for 20 Jan 2004.*

represented in the NAM as compared to the GFS. However, the upper level divergence is often weaker than observed, and only slightly stronger than the GFS (Fig. 8). In addition, the low level convergence within the deformation axis on the northeast quadrant of the short wave is weaker than observed (Fig. 9).

With respect to the cold pool aloft, the NAM does a decent job of forecasting the location. Like the GFS, it is important to focus on the where the cold pool moves and the temperatures within the cold pool, and not as much on the any derived indices such as LI. LI tends to be higher than the corresponding GFS forecasts, with values near 4 C over the Sierra Front. In contrast, HLTT seems to perform much better (Fig. 10) than LI with

values near 34 C over the Sierra Front. These values become closer to 36 C when the 1 C warm bias of the NAM 500 mb temperature forecast over the Sierra Front is factored in.

When it comes to QPF, the NAM can provide a more detailed forecast when deep moisture is present (March 1, 2004 snowstorm – Brong 2006). However, if moisture and instability are shallow, the NAM convective parameterization will not produce precipitation (Betts, 1996, Betts and Miller, 1986, Janjic, 1994, and Staudenmaier, 1996). If the depth of the instability is less than 290 mb, from the lifted condensation level to the equilibrium level (adjusted to the last model level where the parcel is warmer than the environment), the shallow convective scheme is used. (For a summary of the Betts-Miller-Janjic (BMJ) scheme see Staudenmaier 1996, with the complete description of the scheme found in Betts, 1986, Betts and Miller, 1986 and Janjic, 1994). For example, using the 21h NAM forecast sounding for 09 UTC 20 Jan (Fig. 11), the instability is shallow even when adjusted for the cold bias in the surface temperatures. The modified sounding for a temperature of 2 C and a dewpoint of 1 C shows a cloud base below 800 mb, but the equilibrium level is still only at 600 mb. With the convective cloud depth less than 290 mb, the shallow convective scheme is used and no convective precipitation is generated. With no convective precipitation generated, only the grid-scale precipitation is produced, and the rates may be much lighter than what will be observed.

In Fig. 12, the 6-hr and 12-hr precipitation accumulation from the NAM are shown where very light QPF is forecast in the Sierra foothills, with most of the QPF focused on the south end of the Sierra Front. While the heaviest amounts at the south end of the Sierra Front were on the right track, moderate precipitation also occurred further upstream in Reno and Spanish Springs, NV. In addition, the overall QPF was much too light and even performed worse than the GFS as all amounts were less than one tenth of an inch. To reiterate, it was this event that produced over 0.5" of rain at the Reno airport with 10 inches of snow around Topaz Lake. Thus the NAM shows the same dry bias that the GFS does, and QPF amounts in most cases should be doubled at a minimum, especially if the dynamics are stronger than normal, or the instability associated with the inside slider short wave is deep, but not deep enough to trigger the deep convective scheme of the NAM.

IV - Observational Clues

Before the inside slider enters northwest Nevada or northern California, there are often observational clues upstream that will help make any adjustments to model forecasts. Satellite and radar imagery as well as observed soundings are extremely helpful in assessing the strength and coverage of an inside slider event.

a) Satellite and Radar Imagery

Water vapor imagery is extremely helpful in assessing model initialization and forecasting of the inside slider short wave and jet streak (Fig. 13). The usefulness of water vapor imagery to detect mesoscale features is well documented in the literature (Bosart, 2003 is one recent example). On 20 Jan, it is easy to see the location of the main

short wave that will move into western Nevada is near the mouth of the Columbia River. However, both water vapor imagery and infrared imagery are both useful in detecting any convection upstream, generally over central and western Oregon and Washington. Satellite imagery is often the greatest asset over central Oregon due to poor radar coverage in this area. In all cases involving a significant inside slider event, scattered convection was observed upstream over central or western Oregon (Fig. 14). In addition, if any precipitation was observed east of the Cascades, a look at the individual observations will give a clue as to the intensity of the upstream precipitation, and can be used to supplement the model forecast QPF. For example, observed rainfall totals in south central Oregon were up to a quarter inch on 19 Jan, with hourly rates as high as one tenth of an inch.

b) Upper Air Observations

Upper air observations, both upstream and at KREV (Reno, NV), are very helpful in determining the thermodynamic environment both within the inside slider short wave and ahead of it. The Reno sounding is useful, as it will be easy to see if there is a conditionally unstable layer of the atmosphere ahead of the short wave. If there is, there will be a greater potential for convective precipitation and therefore heavier rainfall and/or snowfall rates. This is especially true if the short wave brings in low level moisture (850-700 mb). An example is shown in Fig. 15, and is from 20 Sep 2004. Notice the moist adiabatic temperature profile above the cloud base near 700 mb. This moist adiabatic profile extends upward to almost 300 mb. While this is a case from early fall when the instability is relatively deep, the temperature profile for mid-winter cases is similar, except the moist-adiabatic layer is shallower, and may not extend above 500 mb.

Assessing the downstream environment is only part of the problem as advection ahead of the wave may change the thermodynamic environment. In addition, there will be times where the Reno, NV upper air observation will not be available, which was the case on 20 Jan. Therefore, observations closer to the inside slider short wave itself will give a better representation of the environment the short wave is working on.

Upstream of Reno, NV, the upper air observation sites are Medford and Salem in Oregon, Boise in Idaho and Quillayute and Spokane, WA. In most cases, the Oregon stations are preferred since they are closer to the Sierra Front. However, all of these sites are much lower in elevation than Reno (el. 4450 feet above sea level) so attention should be focused on those levels above 850 mb (slightly less than the station pressure at KREV.) Similar to the KREV observations, conditionally unstable layers should be looked for. In some cases (Fig. 16), the soundings near the short wave itself will show convective available potential energy (CAPE) and little if any convective inhibition (CIN), and exhibits the convective nature close to the track of the inside slider short waves. For Spokane (KOTX), the temperature profile becomes nearly moist adiabatic above 800 mb at 00Z 20 Jan, and the isothermal layer from the 12Z 19 Jan sounding is no longer present. In the KBOI soundings, the profile is also nearly moist adiabatic although there is a shallow isothermal layer near 700 mb.

V - Summary

Inside sliders can be difficult to forecast due to their small size. Both the GFS and NAM will forecast the large scale features of inside sliders such as jet streaks and long wave troughs, but struggle with the mesoscale details of inside sliders. These details include the north to northeast upslope flow along the Sierra Front of western Nevada and any weak convergence zone that may form upstream of the Carson Range due to weak 'barrier jets'. In addition, due to the convective nature of inside sliders, if the model convective schemes are not triggered and/or do not produce precipitation the resulting QPF fields can be much less than what is observed. Therefore, it is important that the forecaster pay close attention to upstream observations and any hints in these observations, including those from satellite, radar and upper air. This way, the forecaster may be able to anticipate inside slider behavior based on the generic inside slider model in Part I, and make the necessary adjustments to the model forecasts.

References

Betts, A.K. 1986: **A new convective adjustment scheme. Part I: Observational and theoretical basis.** *Quart. J. Roy. Meteor. Soc.*, 112, 677-691.

Betts, A.K. and M.J. Miller, 1986: **A new convective adjustment scheme. Part II: Single column tests using GATE wave, BOMEX, and arctic air-mass data sets.** *Quart. J. Roy. Meteor. Soc.*, 112, 693-709.

Bosart, L. F., 2003: **Whither the weather analysis and forecasting process?** *Weather and Forecasting:* Vol. 18, No. 3, pp. 520-529.

Brong, B., 2006: **Microphysical Processes and the Reno Snow Storm on March 1st, 2004.** *Western Region Technical Attachment No. 06-01*. January 24, 2006.

Janjic, Z.I., 1994: **The step-mountain eta coordinate model: Further developments of the convection, viscous sublayer, and turbulence closure schemes.** *Mon. Wea. Rev.*, 122, 927-945

Milne, R., 2004: **A modified Total Totals Index for thunderstorm potential over the Intermountain West**. *Western Region Technical Attachment No. 04-04.* June 15, 2004.

NOAA-EMC, 2003: **The GFS Atmospheric Model.** *NCEP Office Note No. 442.* [http://www.emc.ncep.noaa.gov/officenotes/newernotes/on442.pdf]

Staudenmaier, M. J., 1996: **The convective parameterization scheme in the MesoEta Model.** *Western Region Technical Attachment No. 96-24.* September 17, 1996.

Steenburgh, W. J., 2003: **One hundred inches in one hundred hours: Evolution of a Wasatch Mountain winter storm cycle.** *Weather and Forecasting*: Vol. 18, No. 6, pp. 1018–1036.

Wallmann, J., 2006: **Inside Sliders. Part I: Their features and their effects on the Sierra Front of Western Nevada.** *Western Region Technical Attachment No. 06-02.*

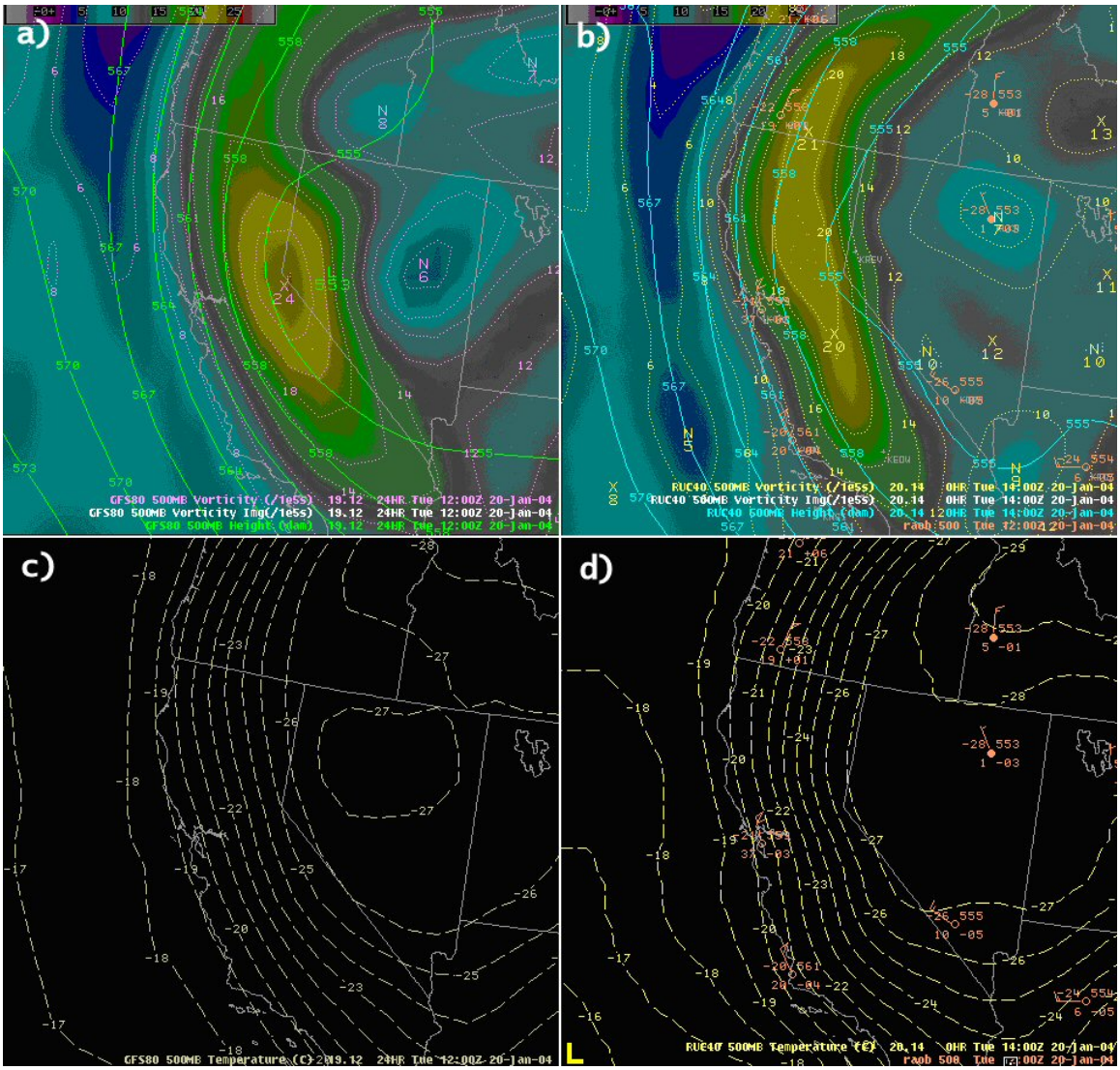

Figure 1. 24 hour forecast from the GFS initialized at 12 UTC 19 Jan 2005 compared with 12 UTC 20 Jan 500 mb upper air plot and 14 UTC 20 Jan RUC40 Analyses. a) GFS 24 hour forecast of 500 mb heights and vorticity. b) 500 mb upper air plot and RUC40 analysis of 500 mb heights and vorticity. c) GFS 24 hour forecast of 500 mb temperature. d) 500 mb upper air plot and RUC40 analysis of 500 mb temperature.

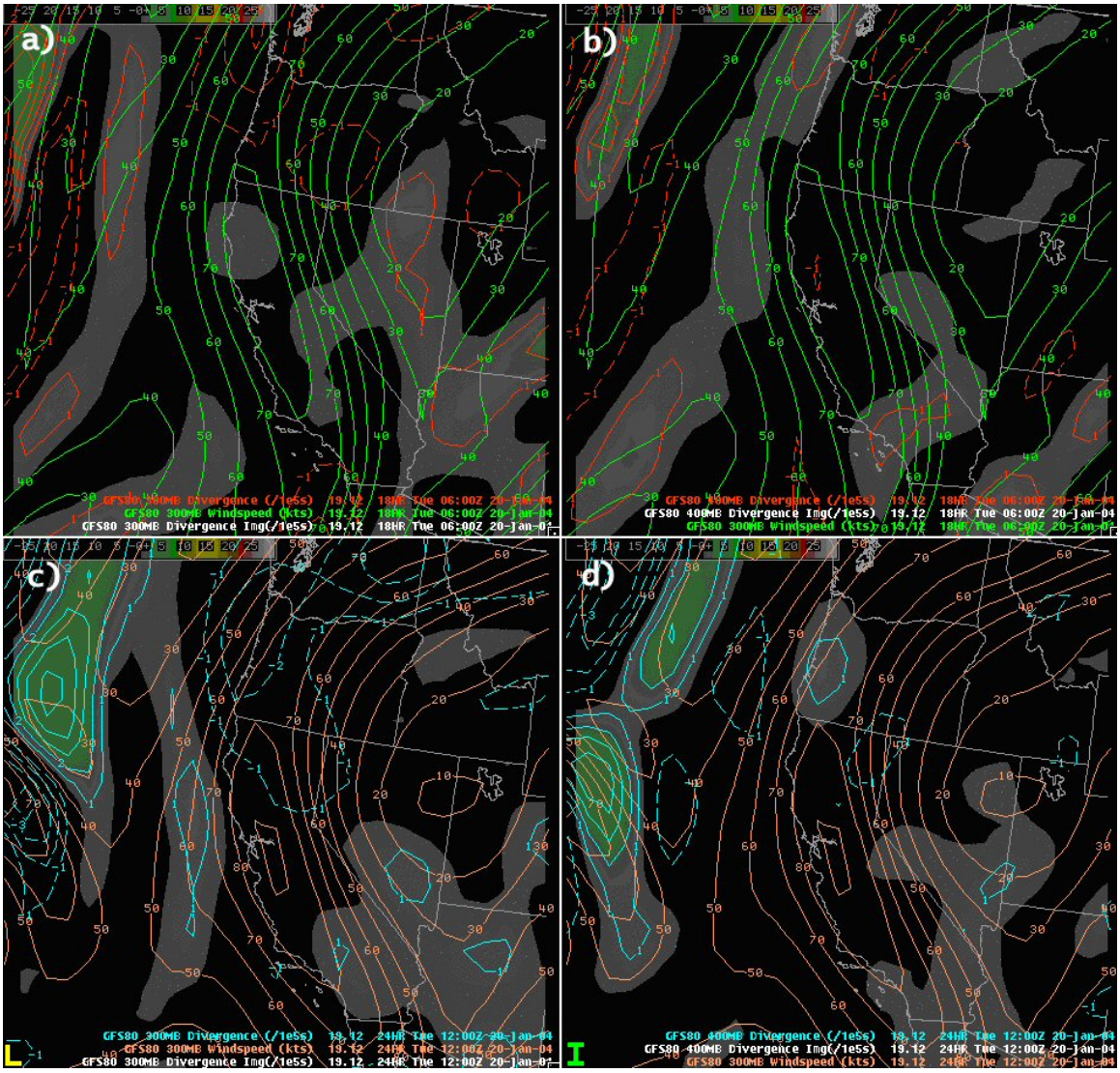

Figure 2. Forecast from the GFS initialized at 12 UTC 19 Jan 2005. a) 18 hour forecast of 300 mb wind speed and divergence (positive values shaded). b) 18 hour forecast of 300 mb wind speed and 400 mb divergence (positive values shaded). c) and d) Same as a) and b), respectively, except the 24 hour GFS forecast.

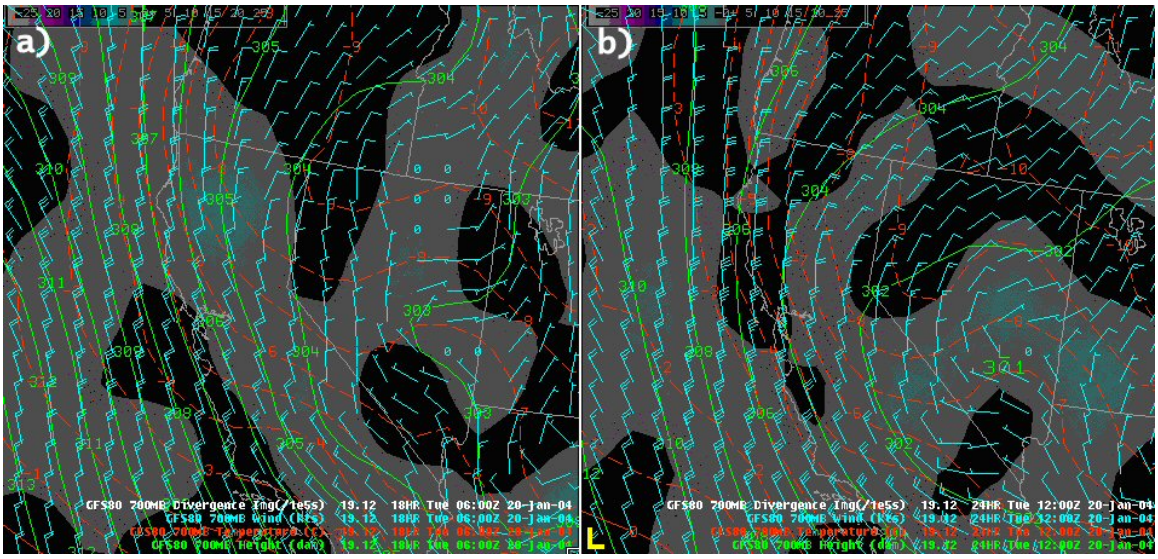

Figure 3. GFS Forecast initialized at 12 UTC 19 Jan 2005. a) 18 hour forecast of 700 mb heights, winds and divergence (negative values shaded indicating convergence). b) 24 hour forecast, same as a).

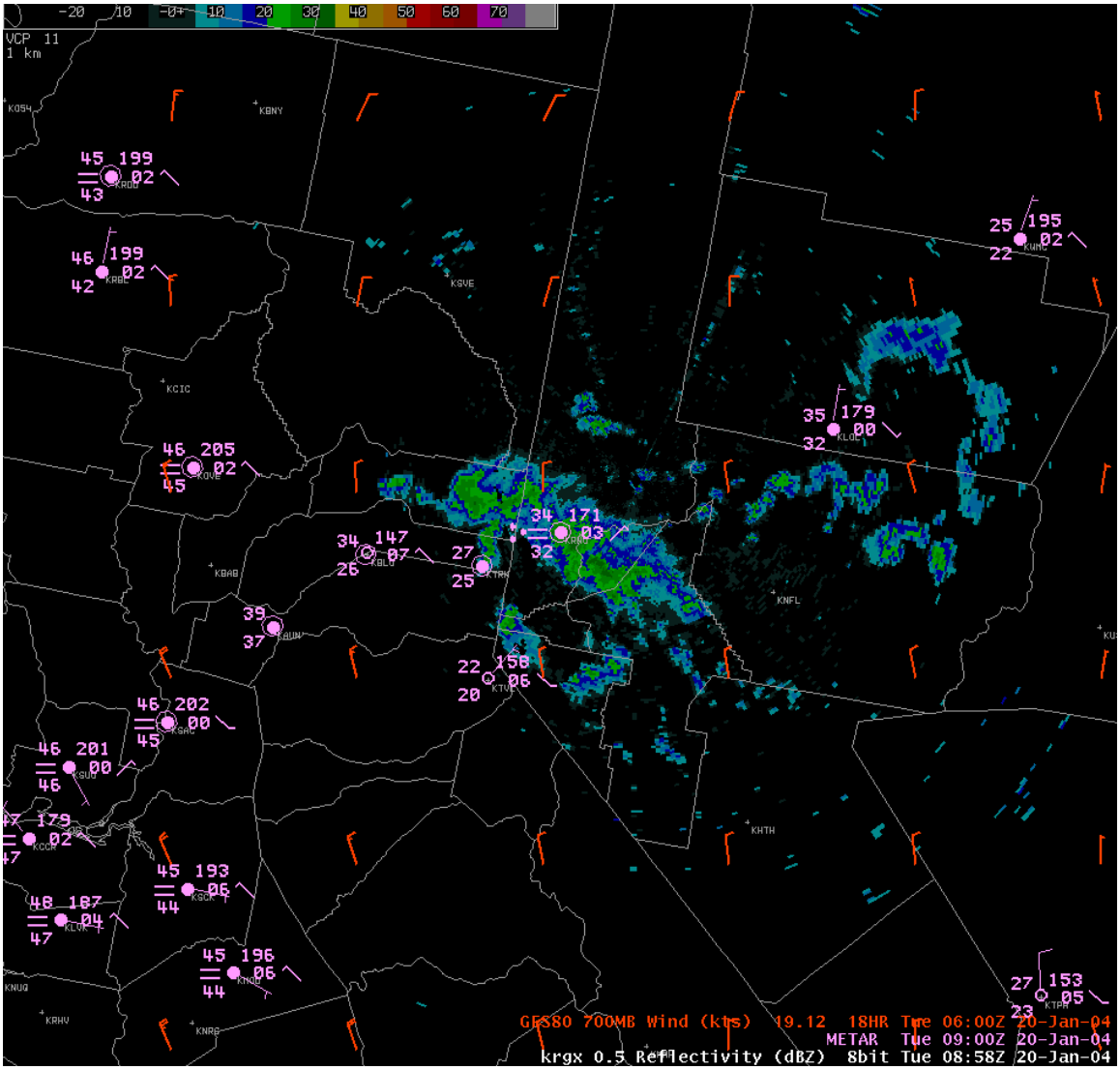

Figure 4. KRGX 0.5 reflectivity at 0904 UTC 20 Jan overlayed with 09 UTC METAR observations.

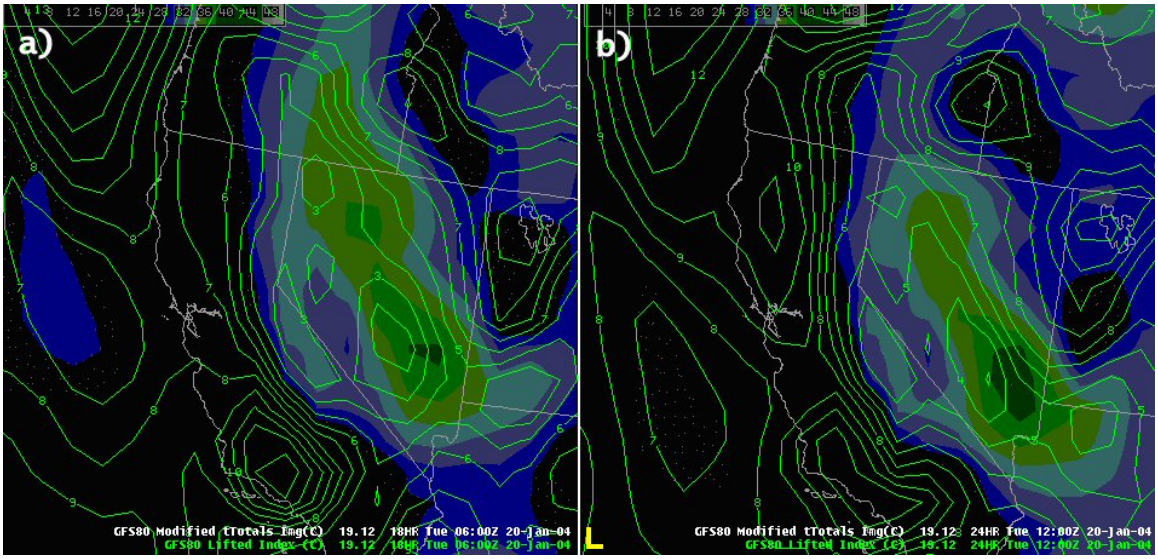

Figure 5. GFS forecast initialized at 12 UTC 19 Jan 2004. a) 18 hour forecast of LI and HLTT (values greater than 28 shaded, with values greater than 34 shaded green.) b) 24 hour forecast, same as a).

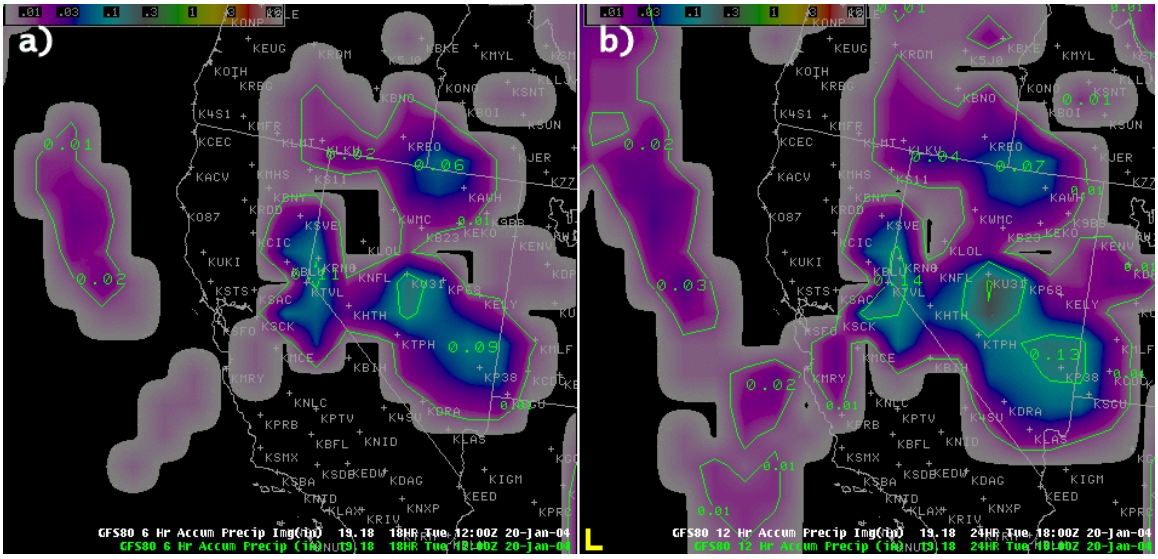

Figure 6. GFS forecast initialized at 18 UTC 19 Jan 2004. a) 6 hour precipitation forecast ending at 12 UTC 20 Jan. b) 12 hour precipitation forecast ending at 18 UTC 20 Jan.

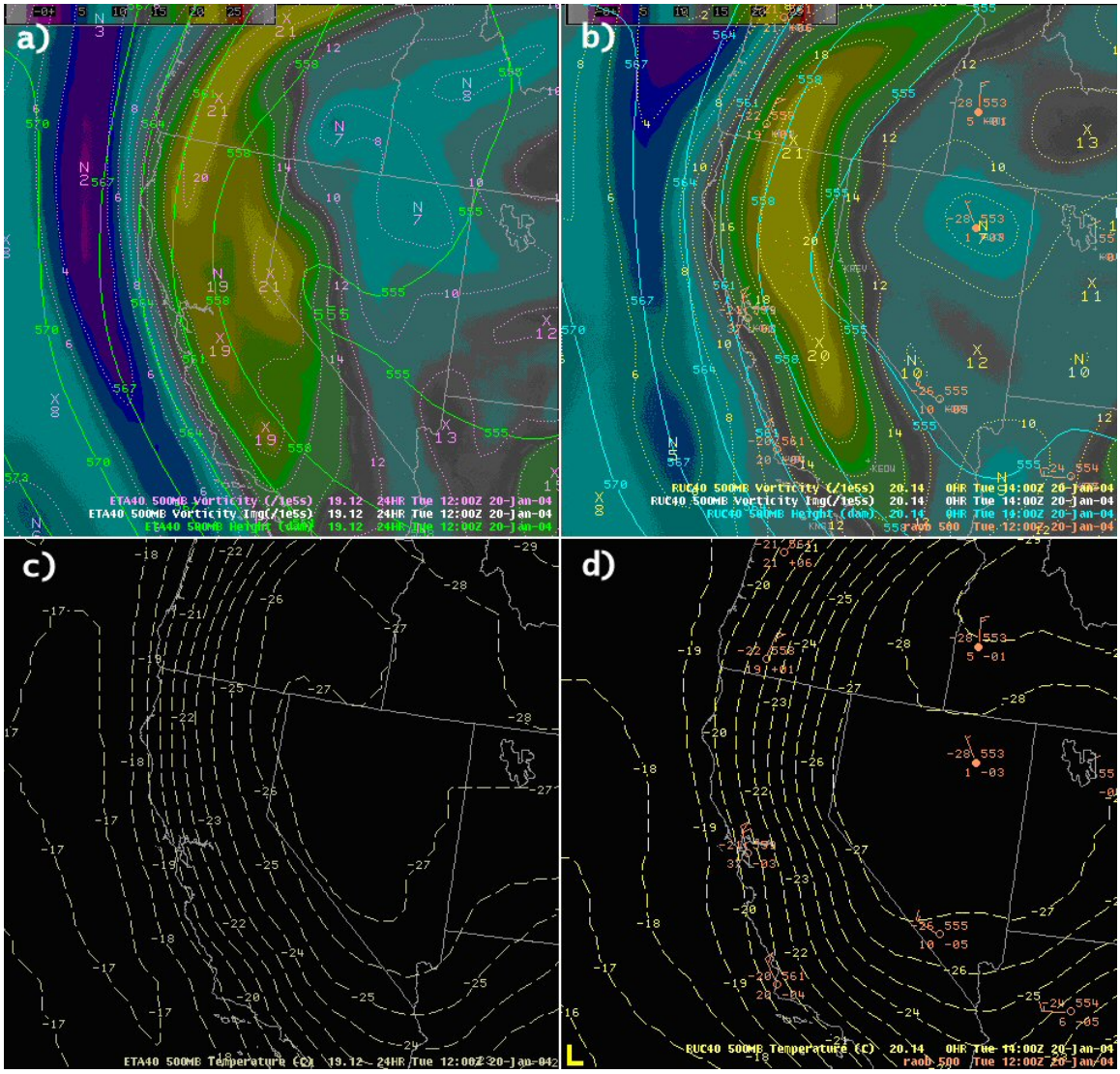

Figure 7. 24 hour forecast from the NAM initialized at 12 UTC 19 Jan 2005 compared with 12 UTC 20 Jan 500 mb upper air plot and 14 UTC 20 Jan RUC40 Analyses. a) NAM 24 hour forecast of 500 mb heights and vorticity. b) 500 mb upper air plot and RUC40 analysis of 500 mb heights and vorticity. c) NAM 24 hour forecast of 500 mb temperature. d) 500 mb upper air plot and RUC40 analysis of 500 mb temperature**.**

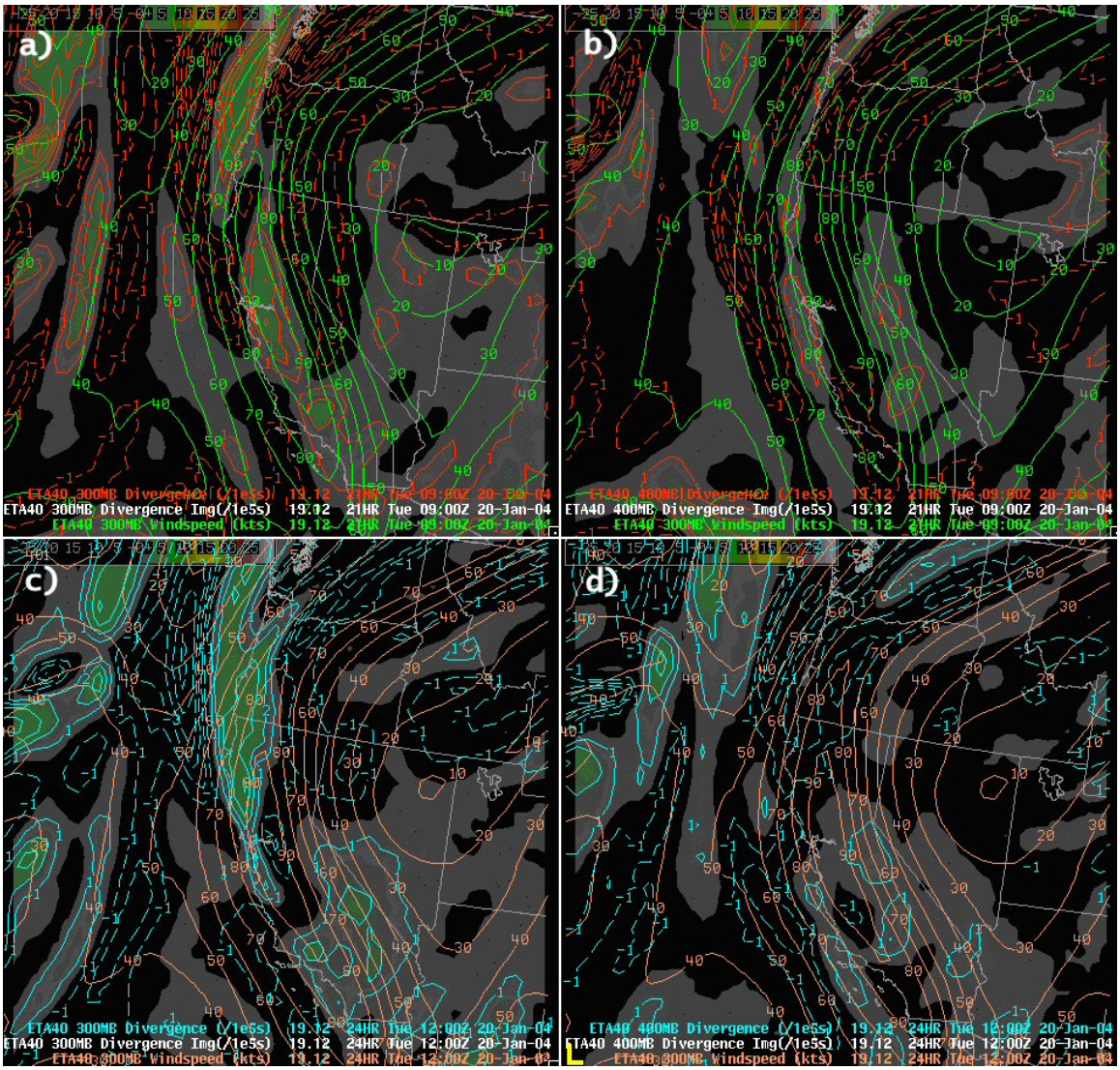

Figure 8. Forecast from the NAM initialized at 12 UTC 19 Jan 2005. a) 21 hour forecast of 300 mb wind speed and divergence (positive values shaded). b) 21 hour forecast of 300 mb wind speed and 400 mb divergence (positive values shaded). c) and d) Same as a) and b), respectively, except the 24 hour NAM forecast.

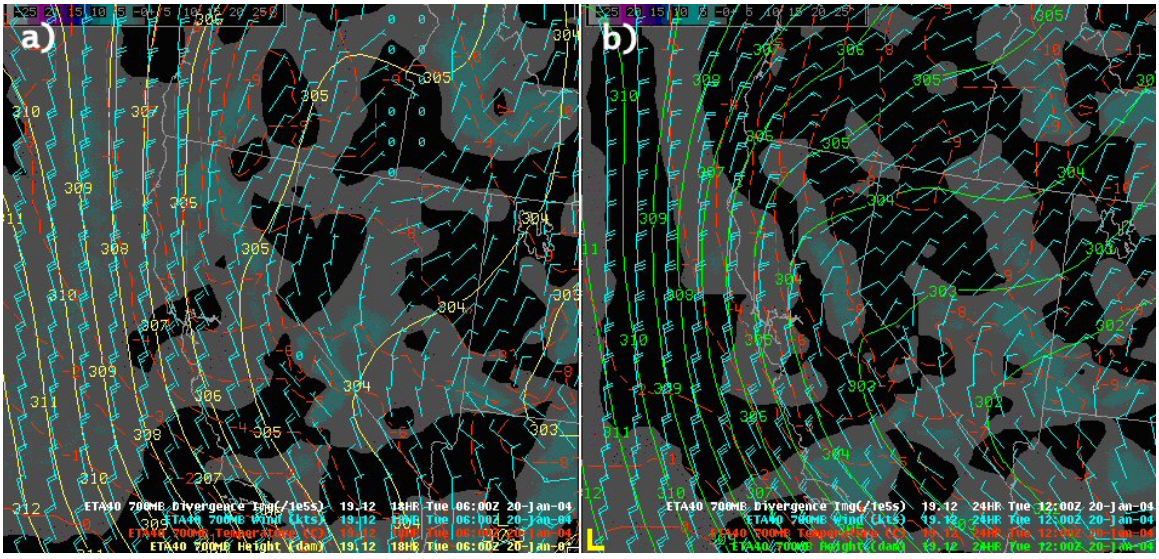

Figure 9. NAM Forecast initialized at 12 UTC 19 Jan 2005. a) 18 hour forecast of 700 mb heights, winds and divergence (negative values shaded indicating convergence). b) 24 hour forecast, same as a).

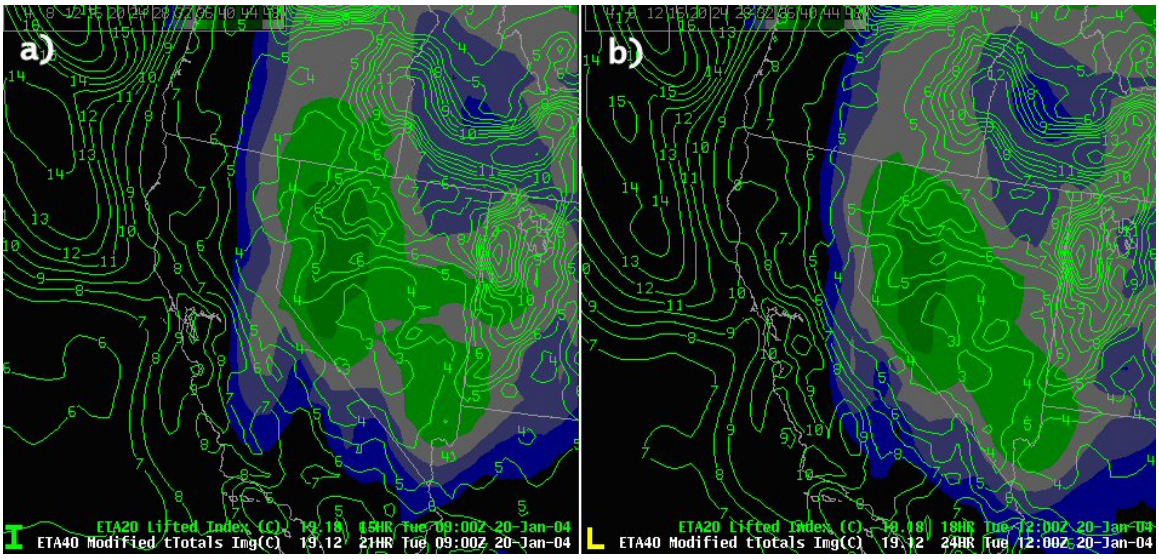

Figure 10. NAM forecast initialized at 12 UTC 19 Jan 2004. a) 18 hour forecast of LI and HLTT (values greater than 28 shaded, with values greater than 34 shaded green.) b) 24 hour forecast, same as a).

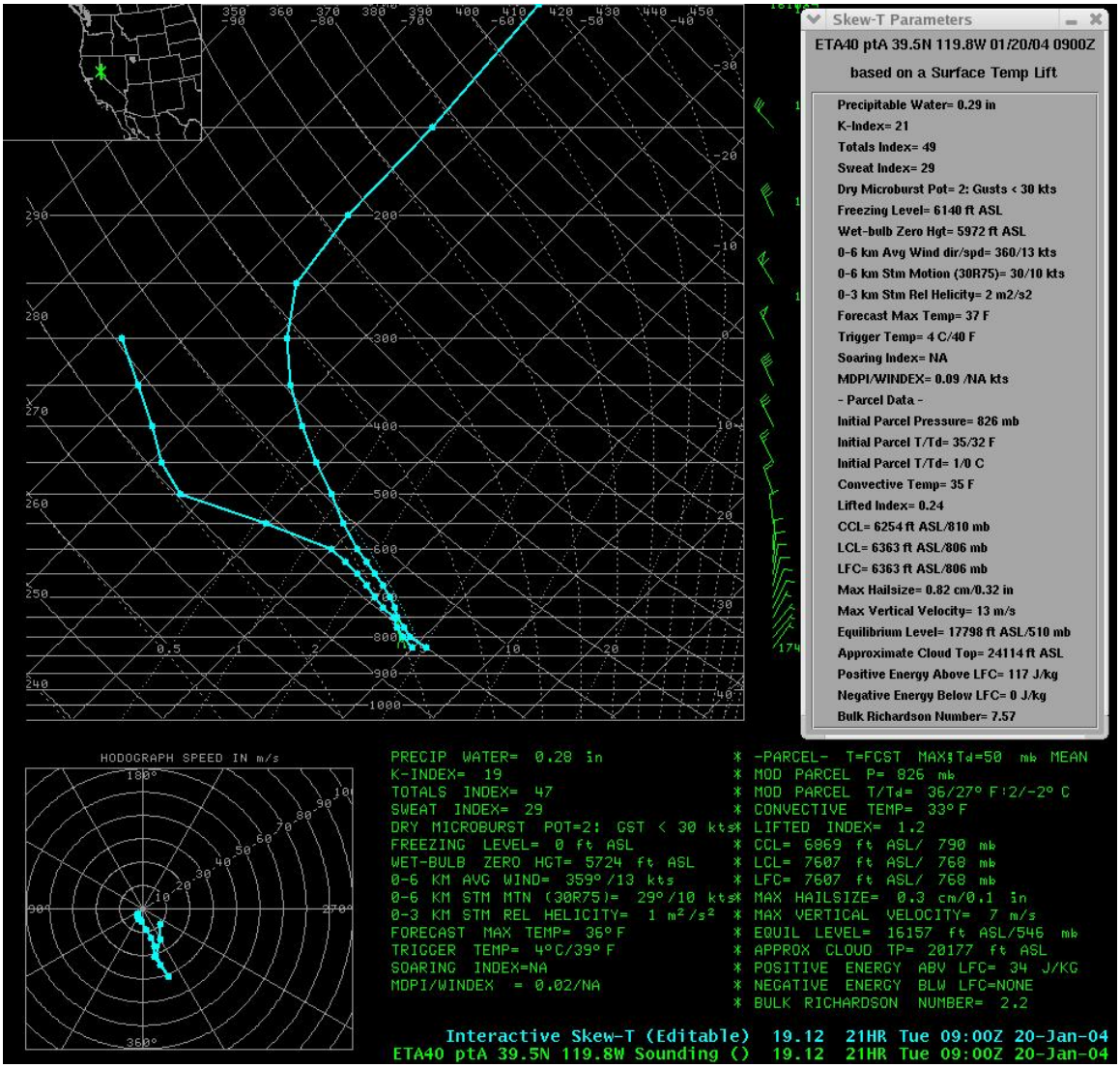

Figure 11. 12 UTC 19 Jan NAM40 forecast sounding for KRNO verifying at F21 – 09 UTC 20 Jan.

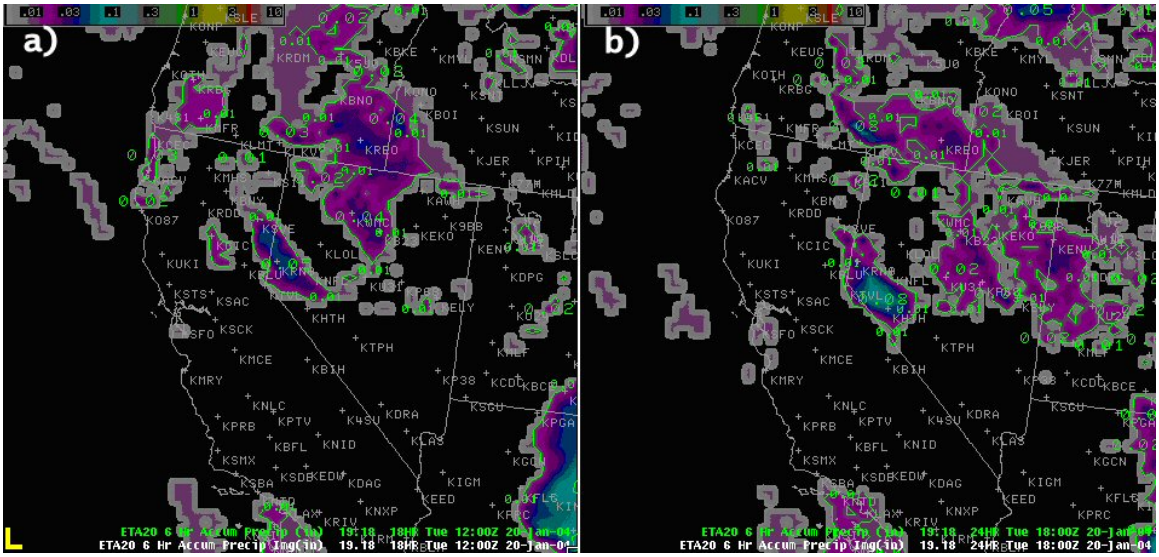

Figure 12. Precipitation forecast from the NAM initialized at 18 UTC 19 Jan 2005. a) 6 hour forecast ending 12 UTC 20 Jan. b) 6 hour forecast ending 18 UTC 20 Jan.

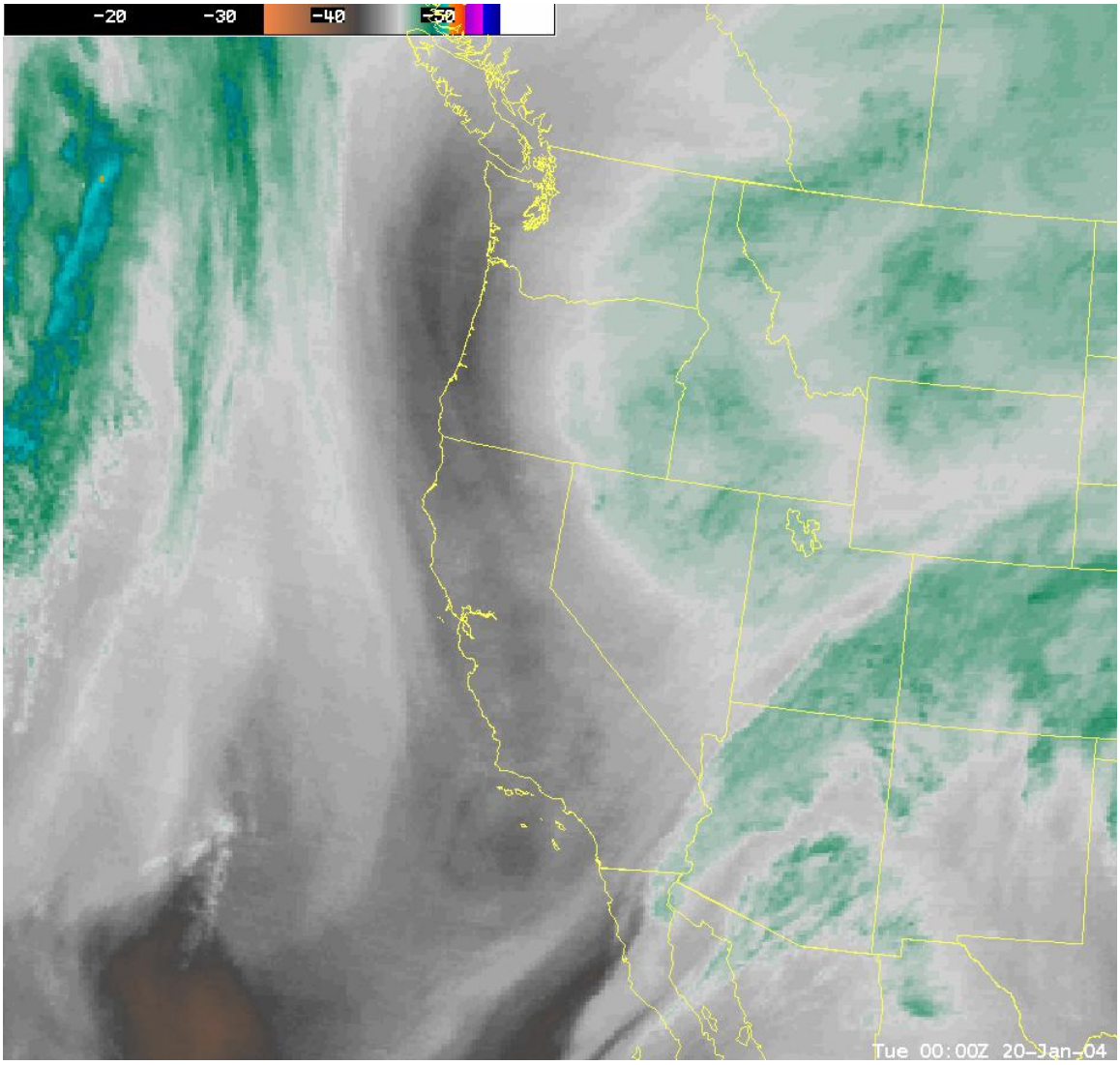

Figure 13. Water vapor channel satellite image at 00 UTC 20 Jan 2004.

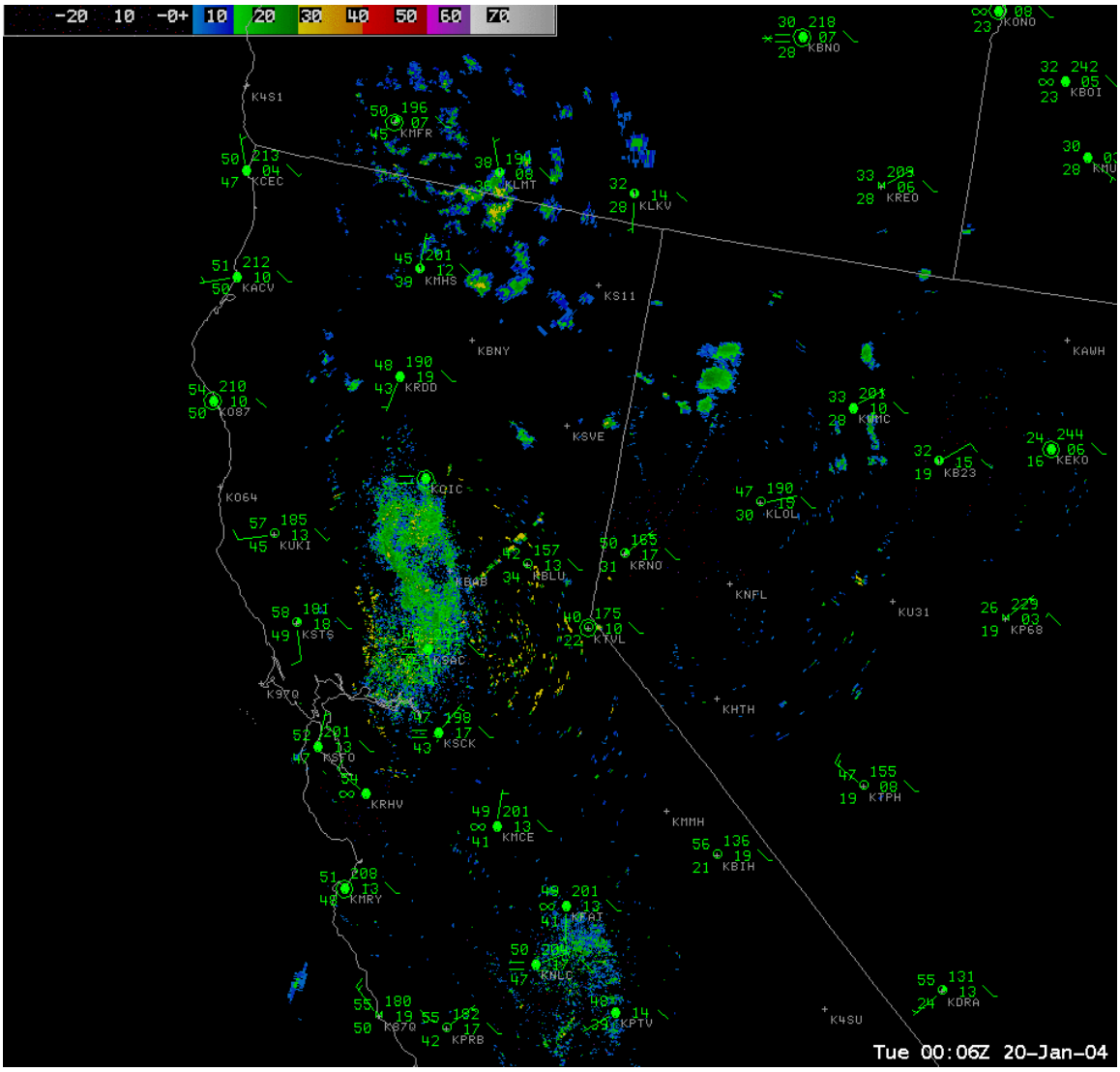

Figure 14. WSR-88D 0.5 reflectivity mosaic at 0006 UTC 20 Jan 2004 with METAR plot from 00 UTC.

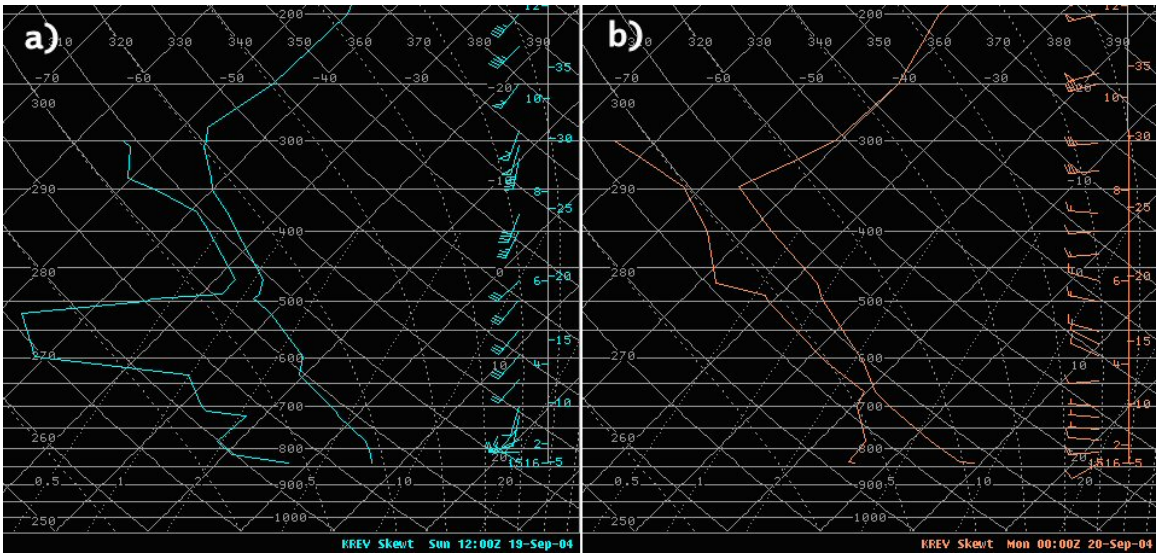

Figure 15. a) 12 UTC 19 Sep 2004 upper air sounding from KREV (Reno, NV). b) 00 UTC 20 Sep upper air sounding from KREV.

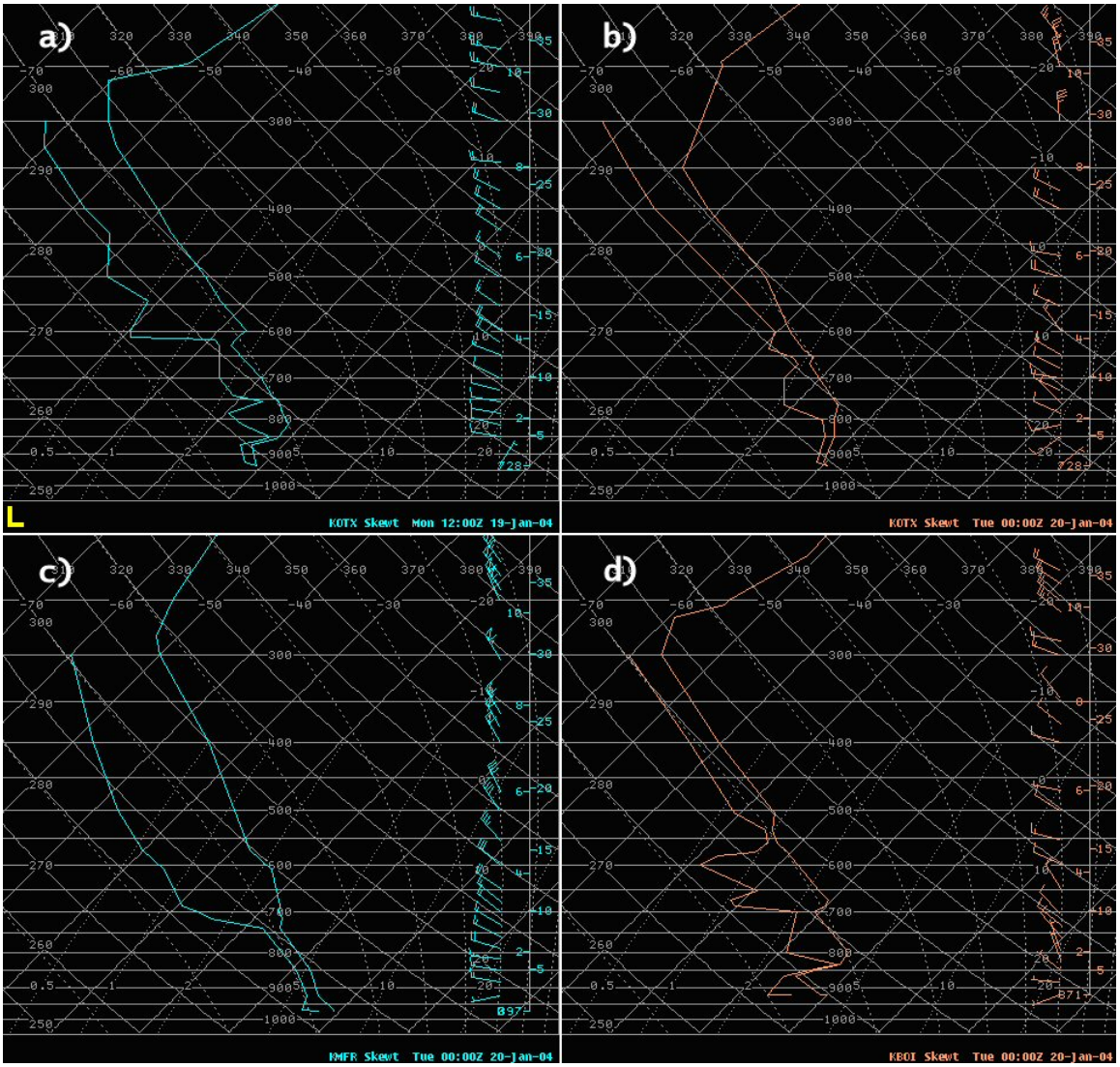

Figure 16. a) 12 UTC 19 Jan 2004 upper air sounding from KOTX (Spokane, WA). b) 00 UTC 20 Jan 2004 upper air sounding from KOTX. c) 00 UTC 20 Jan upper air sounding from KMFR (Medford, OR). d) 00 UTC 20 Jan upper air sounding from KBOI (Boise, ID).